Simultaneous Detection of Circularly Polarized Luminescence and Raman Optical Activity in an Organic Molecular Lemniscate

Luis Palomo, Ludovic Favereau, Kabali Senthilkumar, Marcin Stepien, Juan Casado, Francisco J. Ramírez

▶ **To cite this version:**

Luis Palomo, Ludovic Favereau, Kabali Senthilkumar, Marcin Stepien, Juan Casado, et al.. Simultaneous Detection of Circularly Polarized Luminescence and Raman Optical Activity in an Organic Molecular Lemniscate. Angewandte Chemie International Edition, 2022, 61 (34), pp.-e202206976. 10.1002/anie.202206976 . hal-03772724

HAL Id: hal-03772724
https://hal.science/hal-03772724

Submitted on 17 Feb 2023

HAL is a multi-disciplinary open access archive for the deposit and dissemination of scientific research documents, whether they are published or not. The documents may come from teaching and research institutions in France or abroad, or from public or private research centers.

L'archive ouverte pluridisciplinaire **HAL**, est destinée au dépôt et à la diffusion de documents scientifiques de niveau recherche, publiés ou non, émanant des établissements d'enseignement et de recherche français ou étrangers, des laboratoires publics ou privés.

Check for updates

How to cite: *Angew. Chem. Int. Ed.* **2022,** *61,* e202206976
International Edition: doi.org/10.1002/anie.202206976
German Edition: doi.org/10.1002/ange.202206976

Chirality

Simultaneous Detection of Circularly Polarized Luminescence and Raman Optical Activity in an Organic Molecular Lemniscate

Luis Palomo, Ludovic Favereau, Kabali Senthilkumar, Marcin Stępień, Juan Casado, and Francisco J. Ramírez**

Abstract: Circularly polarized luminescence (CPL) and Raman optical activity (ROA) were observed in a single spectroscopic experiment for a purely organic molecule, an event that had so far been limited to lanthanide-based complexes. The present observation was achieved for [16]cycloparaphenylene lemniscate, a double macrocycle constrained by a rigid 9,9′-bicarbazole subunit, which introduces a chirality source and allows the molecule to be resolved into two configurationally stable enantiomers. Distortion of oligophenylene loops in this lemniscular structure produces a large magnetic transition dipole moment while maintaining the π-conjugation-induced enhancement of the Raman signal, causing the appearance of the CPL/ROA couple. A two-photon mechanism is proposed to explain the population of the lowest-energy excited electronic state prior to the simultaneous emission-scattering event.

Chirality, a ubiquitous property in Nature, is found at all size scales of matter, ranging from atomic particles to galaxies. In organic molecules, chirality is usually associated with the presence of an asymmetric carbon atom, although polycyclic aromatic molecules can also become chiral when distorted into stable twisted or helical shapes. A special case of this chirality type is found in the recently reported [16]cycloparaphenylene lemniscate ([16]CPPL, Figure 1),[1,2] a cycloparaphenylene[3] derivative in which the chiral configuration is stabilized by a rigid 9,9′-bicarbazole moiety, enabling separation of enantiomers.[1,2] [16]CPPL combines chirality with radial π-conjugation, a characteristic feature of aromatic nanohoops and nanobelts that is responsible for their unusual photophysical and optoelectronic properties.[3b,4]

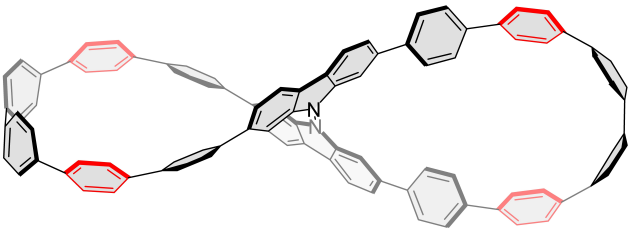

Figure 1. Molecular structure of [16]cycloparaphenylene lemniscate ([16]CPPL) studied in this work.

Raman spectroscopy has proven to be an advantageous tool for probing electronic properties of π-conjugated molecules. Its utility stems from the well-established electron-vibration coupling, which makes the C–C/C=C stretching bands good markers of π-electron features.[5–7] Raman optical activity (ROA) is the chiral version of Raman spectroscopy. It measures the optical activity of a chiral system using either scattered circular polarization (SCP-ROA), i.e. by subtracting the intensities of the right and left circularly polarized scattering, or incident circular polarization (ICP-ROA), achieved by appropriate modulation of the laser source.[8–11] Given that out-of-plane distortions of the core in π-conjugated systems (see relative angles between benzenes in [16]CPPL in Figure 1) promote increasing contributions of the magnetic transition dipole moments to the overall activity of electronic and vibrational spectral bands, with ROA spectroscopy one can establish unique relationships between the magnetic contribution of the π-electronic response and the geometrical distortions of a chiral π-conjugated system (i.e., often this is extracted from the analysis of the electrical part of the electric transition dipole moment).

Circularly polarized luminescence (CPL) accounts for the capacity of a chiral molecule in an excited electronic state to emit left and right circularly polarized photons.[12] CPL further permits analyzing optical activity of transitions not easily observable in common absorption bands, such as singlet–triplet excitations in organic molecules or *f–f* transitions of lanthanide-based systems.[13]

[*] L. Palomo, Prof. J. Casado, Prof. F. J. Ramírez
Department of Physical Chemistry, Faculty of Sciences, University of Málaga
Campus de Teatinos, 29071 Málaga (Spain)
E-mail: casado@uma.es
ramirez@uma.es

Dr. L. Favereau
Univ Rennes, CNRS
ISCR—UMR 6226, 35000 Rennes (France)

Dr. K. Senthilkumar, Prof. M. Stępień
Wydział Chemii, Uniwersytet Wrocławski
ul. F. Joliot-Curie 14, 50-383 Wrocław (Poland)

© 2022 The Authors. Angewandte Chemie International Edition published by Wiley-VCH GmbH. This is an open access article under the terms of the Creative Commons Attribution Non-Commercial NoDerivs License, which permits use and distribution in any medium, provided the original work is properly cited, the use is non-commercial and no modifications or adaptations are made.

© 2022 The Authors. Angewandte Chemie International Edition published by Wiley-VCH GmbH

The presence of fluorescence in a Raman experiment deteriorates the intensity of the scattered signal and is thus normally an unwanted effect. Nevertheless, in chiral molecules, simultaneous occurrence of CPL and ROA effects might be beneficial, as it can provide additional insight into electronic properties of enantiopure chromophores. However, given their competing requirements, CPL and ROA are extremely difficult to detect in a single spectroscopic experiment. Such double detection has so far only been reported for molecular lanthanide complexes, which benefit from high magnetic dipole moments associated to the *f*–*f* electronic transitions, whose excitation energies lie in the mid-infrared range, thus allowing to be detected in a ROA experiment together with the vibrational bands of the organic moiety.[14–15] Here we show that CPL and ROA can be simultaneously detected in [16]CPPL, providing the first instance of such an observation in a purely organic system. Such experiments are challenging because magnetically controlled excitations are typically concealed by those triggered by the electric field and, furthermore, the former are extremely weak in organic molecules containing only light atoms. In [16]CPPL, however, the unique distortion of the π-system provides an alternative basis for enhancement of magnetically controlled excitations, enabling simultaneous observation of the CPL-ROA couple.

Figure 2 shows the SCP-ROA spectra of (*M*)- and (*P*)-enantiomers of [16]CPPL. The presence of negative and positive vibrational ROA bands, and the markedly different profiles of ROA and Raman spectra (Raman spectra of [16]CPPL are shown in Figure S1) rule out resonant scattering. The (*P*)- and (*M*)- enantiomers exhibit specular ROA spectra in the whole mid-IR vibrational region. Both the signs and the wavenumbers of the main observed bands were reproduced by the computationally predicted ROA spectra, thus confirming the experimental spectra were recorded in far-from-resonance settings. Meeting the latter condition was crucial because the exclusion of optical (electric field) enhancements in the ROA spectra is necessary to assess the magnetically driven electronic & vibrational transitions that produce, respectively, the CPL and ROA spectra.

Bands were assigned on the basis of the calculated vibrational eigenvalues and the group coupling matrix method proposed by Hug[16,17] (see Figures S2–S4). The more intense features in the 1550–1650 cm^{-1} range correspond to aromatic C–C stretching vibrations of i) the bicarbazole group (i.e., the bisignate signal at higher wavenumbers), and ii) the oligophenylene moieties (the bands at lower wavenumbers). The ROA activity of this bisignate is also due to the bicarbazole moiety, while the contribution of the oligophenylene loops originates mostly from the interaction terms with the bicarbazole group. The latter relationship rationalizes the low vibrational amplitude of the bicarbazole-attached phenylenes in the related eigenvalues. The two components of the strongest bisignate at 1280 cm^{-1} are mostly assigned to skeletal vibrations of the bicarbazole group.

In Figure 3, the Raman and ROA spectra of the two enantiomers of [16]CPPL are superimposed onto the corresponding fluorescence and CPL spectra, to show that the Raman/ROA fingerprints overlap with the low-energy tails of the fluorescence/CPL spectra (540–610 nm), which correspond to the 0–*n* vibronic progression of the $S_1 \rightarrow S_0$ electronic transition. This was essential to detect both emission and scattering events together, as overlapping near the maximum fluorescence efficiency region would produce saturation of the scattered radiation over the Raman detector, thus preventing the resolution of good-quality ROA spectra. Importantly, the ROA backgrounds are flipped upside down with respect to the corresponding vibronic band of the CPL experiment, whose sign coincides with that of the lowest energy electronic circular dichroism (ECD) feature, $S_0 \rightarrow S_1$. To interpret this result, we must take into account the opposite definitions adopted for vibrational (i.e I_R–I_L for infrared and Raman) and electronic (i.e., I_R–I_L for absorption and fluorescence) circular dichroisms,[17,18] which allow us to assign these spectroscopic correlations to a simultaneous detection of CPL and ROA spectra in a single

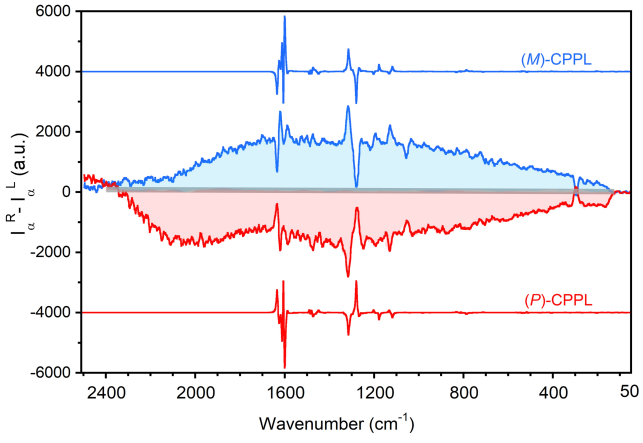

Figure 2. Middle: SCP-ROA spectra of (*M*)- and (*P*)- enantiomers of [16]CPPL in dichloromethane solutions. Top and bottom: theoretical ROA spectra. The intensity scale corresponds to the experimental spectra.

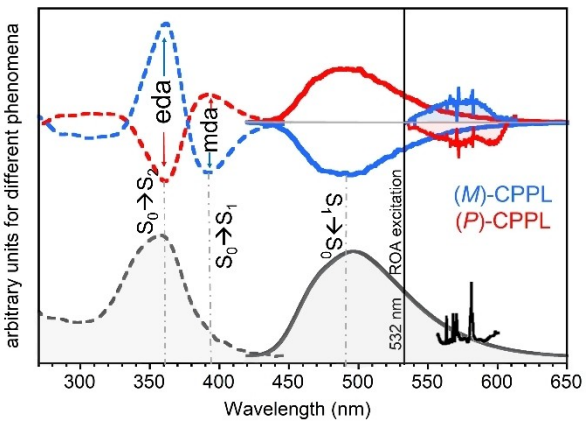

Figure 3. Absorption, fluorescence and Raman spectra (black lines), ECD, CPL and SCP-ROA spectra (coloured lines), of (*M*)- and (*P*)-enantiomers of [16]CPPL in dichloromethane solutions.

© 2022 The Authors. Angewandte Chemie International Edition published by Wiley-VCH GmbH

spectroscopic experiment. To the best of our knowledge, this is the first time such an observation is made in a purely organic molecule. The present instance seems to originate from the right balance between the Raman/ROA enhancement caused by π-conjugation and the magnetic exaltation effect caused by the curved structure of [16]CPPL.[5]

Circular dichroism features are quantified using the dissymmetry factor, g, which is defined as the ratio between the difference spectral intensity for left and right circularly polarized light, and the intensity obtained for unpolarized radiation at the same energy, either in absorption (g_{abs}) or in emission (g_{lum}). For electronic transitions, g satisfies Equation (1):

$$g = \frac{4|m|}{|\mu|}\cos\theta, \tag{1}$$

where m and μ are the magnetic and the electric transition dipole moments, MTDM and ETDM, respectively, while θ is the angle formed by these two vectors.[12] When applied to CPL spectroscopy, this equation indicates that high g_{lum} values can only result for transitions with a large magnetic dipole moment and a sufficiently small angle between the ETDM and MTDM vectors.

Figure 4 shows the ETDM and MTDM vectors calculated for the most intense electronic transitions of (*M*)-[16]CPPL between 300 and 450 nm (see Supporting Information for computational details, the calculated spectra in Figure S5, and a complete set of ETDM and MTDM components in Tables S1 and S2). The D3 transition (388 nm) exhibits a small MTDM, a high ETDM, and an θ angle of 31.1°. The ECD intensity of any electronic transition $\phi_i \rightarrow \phi_j$ is determined by the rotational strength, R_{ij}, given by the Rosenfeld equation (2):[19]

$$R_{ij} = |\mu_{ij}||m_{ij}|\cos\theta \tag{2}$$

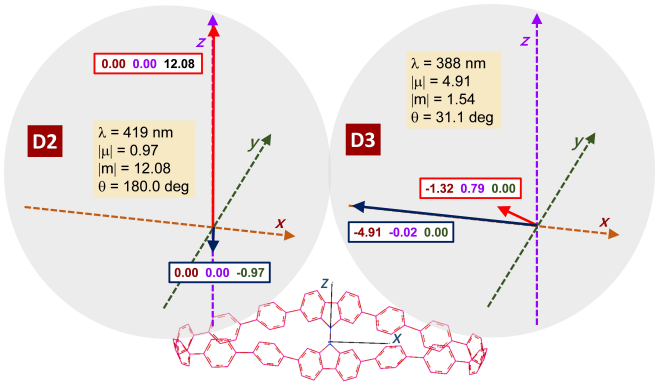

Figure 4. A vectorial representation of ETDM (in 10^{-18} esu cm, blue vectors) and MTDM (in 10^{-21} erg G^{-1}, red vectors) for D2 and D3 electronic transitions of (*M*)- [16]CPPL. The numeric data allow to obtain the rotational strength of each transition (and therefore its ECD intensity) by applying the Rosenfeld equation. The molecular orbitals involved in these transitions are included in Table S3 and Figure S7 of the Supporting Information.

where i and j denote the initial and final electronic states, respectively.

Consequently, the rotational strength of D3 originates from a large ETDM value and a positive cosine, so it can be assigned to the intense positive Cotton effect observed in the ECD spectrum of (*M*)-[16]CPPL centered at 360 nm (which also encloses transitions labelled as D4 and D6 in Figure S6). As an electric dipole allowed (*eda*) transition, it gives rise to an intense band in the absorption spectrum, since it is only driven by the electric dipole mechanism. Conversely, D2 (419 nm) involves a high MTDM and a small ETDM, with a θ angle of 180°. It is therefore a magnetic dipole allowed (*mda*) transition, clearly identified as a negative ECD feature (Figure 3). However, its low ETDM makes the D2 transition almost inactive in absorption. According to the Kasha rule,[20] emission takes place from the lowest-energy excited state, which is *mda* active in [16]CPPL, and yields a significant and measurable CPL signal (conversely, *eda* transitions produce weak or no chiral luminescence). The assignment of the ECD/CPL spectra in terms of *eda* and *mda* transitions of the chiral [16]CPPL provides additional insight into the spectroscopic nature of the low-energy lying excitations of achiral [*n*]cycloparaphenylenes ([*n*]CPPs).[3a,21,22] Specifically, the $S_0 \rightarrow S_1$ transition in the absorption spectra of [*n*]CPPs is not only electrically-dipole forbidden by the cyclic symmetry (*eda* forbidden), but it is also allowed by the magnetic-dipole mechanism (i.e., *mda* allowed and detectable in ECD). Additionally, the next higher energy absorption of cycloparaphenylenes ($S_0 \rightarrow S_2$) is *eda* allowed.

For [16]CPPL, the existence of a lowest-energy excited electronic state that can be populated with a 532 nm laser in the ROA experiment, and whose deactivation by fluorescence involves a transition with high MTDM, justifies the simultaneous emergence of CPL and ROA spectra. The measured g_{lum} for the lowest-energy CPL band was 0.003–0.004, i.e., within the 10^{-2}–10^{-3} range usually observed for organic molecules. The ROA dissymmetry factor (circular intensity difference, CID),[16] does not exceed 10^{-3} for most organic systems. These two factors are related by the simple relationship $CID = -(^1/_2)g_{lum}$, in which the minus sign is a consequence of the opposite definitions of electronic and vibrational circular dichroisms. Table 1 summarizes the CID values obtained for the main ROA bands of (*M*)-[16]CPPL. Importantly, for the vibrations belonging to the bicarbazole group, theoretical CID values show very good correlation

Table 1: Circular intensity difference (CID) values measured for the main ROA bands of (*M*)-[16]CPPL. The experimental CID were measured on the spectra in dichloromethane solutions.

ν_{exp} [cm^{-1}]	ν_{calc} [cm^{-1}]	Assignment	exp. CID [10^{-3}]	calc. CID [10^{-3}]
1635	1634	bicarbazole	−1.11	−2.27
1620	1626	bicarbazole	1.17	8.29
1590	1600	oligophenyl	0.41	−58.06
1314	1316	bicarbazole	2.16	16.59
1280	1280	bicarbazole	−1.55	−2.40
1207	1203	oligophenyl	−0.66	−2.17

© 2022 The Authors. Angewandte Chemie International Edition published by Wiley-VCH GmbH

with the experiment, whereas large discrepancies are observed for modes involving oligophenylene chains. This result demonstrates the high sensitivity of chiral signals to conformational changes, which leads to a decrease of intensity for bands associated with more flexible groups. This effect was further confirmed for [16]CPPL by recording its ROA spectra in decalin (see Figure S8), a much more viscous solvent than dichloromethane, in which the oligophenyl ROA bands were enhanced with respect to the bicarbazole ones. The mean absolute CID for the bicarbazole bands in decalin was 1.49×10^{-3}, which is within the range estimated on the basis of g_{lum}.

The ECD spectra of the two enantiomers display negligible rotational strength at the 532 nm wavelength used by the laser source, indicating that the ROA experiment should be free from either resonant or pre-resonant excitation effects. This assumption is in line with the similitude of the theoretical and the experimental far-from-resonance ROA spectra. In addition, the bisignate shape of the ROA spectra and the correct relationships between the g_{lum} and CID values further rule out the interference from possible resonant effects.

As already indicated, the part of the whole CPL spectrum recorded for [16]CPPL in the ROA measurement emerges from a high-energy vibronic progression in the emission. However, this relationship raises the question of how the energetically lowest excited electronic state is populated enough to produce a CPL signal sufficiently strong to be detected in a SCP-ROA experiment. A hypothesis based on a selective excitation of highly planar conformers with negligible absorption in ECD could be supported by the large Stokes shift measured between the ECD and CPL spectra, which implies a large structural difference between the initial Franck–Condon geometry of the S_1 excited state and the relaxed S_1 geometry, from which the $S_1\rightarrow S_0$ emission takes place. This mechanism is represented by box 1 in Figure 5. It has been suggested that, in π-conjugated systems, torsional distortions in the form of fractional or constrained rotations can yield noticeable changes of magnetic dipole moments,[23] thus augmenting the *mda* contributions responsible of a strong CPL emission (S_1 state in Figure 5). A complementary mechanism which would further explain the spectra of Figure 2 involves two-photon excitation (TPE). In this process, the sum of the energies of two identical photons allows the molecule to reach a high energy electronic state, S_n(TPE) in Figure 5. In the first event, 1-photon excitation/dispersion of/from the produced virtual state (i.e., box 2 in Figure 5) gives rise to Raman or ROA scattering. In a second event, a simultaneous second photon through a TPE mechanism excites the molecule to the S_n(TPE) state (i.e., box 3a in Figure 5) which, after non-radiative internal conversion, populates enough the vibrational ground level of the S_1 state to produce an observable fluorescence emission (i.e., box 3b in Figure 5). The feasibility of this TPE mechanism posteriorly producing fluorescence implies the use of an intense monochromatic laser source and an ultra-sensible detector, both implemented in our ROA spectrometer. In our case, the existence of excited states at energies ca. 4.66 eV above the ground state is also required (532 nm is equivalent to 2.33 eV). Quantum chemistry calculations have predicted four excited states whose energies, with respect to the ground state, are between 4.5 and 4.7 eV, which supports the TPE mechanism.

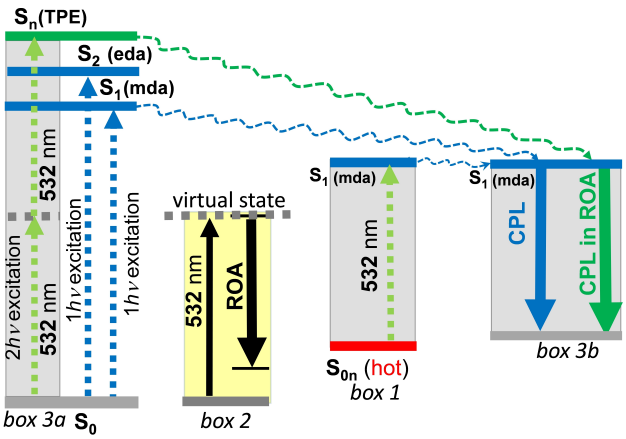

Figure 5. Jablonski diagram including scattering scheme with the electronic, vibronic and vibrational levels involved in the whole CPL (grey boxes 1 and 3a/3b) and ROA (yellow box 2) processes.

In conclusion, we have demonstrated here simultaneous detection of Raman optical activity and circularly polarized luminescence, both emerging from an *mda* mechanism in the same electronic excitation, which are recorded for the first time in a purely organic system. The structural basis for the present observation is proposed to involve the balance between the rigidity of the chiral bicarbazole core of [16]CPPL and the torsional flexibility of the oligophenylene loops. In particular, dynamic distortions of these loops are able to stimulate magnetically allowed transitions which can then be detected by conventional spectroscopic instruments. We have demonstrated the high magnetic dipole moment associated with the deactivation by fluorescence and propose a two-photon absorption as the more likely mechanism to populate this state. The present work offers a new view on magnetically-driven electronic processes in metal-free π-aromatic molecules, an unexplored area in the field of organic materials, which may complement the ongoing research on electrically driven optical phenomena.

Acknowledgements

We thank MINECO/FEDER of the Spanish Government (project reference PGC2018-098533-B-100 and PID2021-127127NB-I00) and the Junta de Andalucía, Spain (UMA18-FEDERJA057). We also thank the vibrational spectroscopy unit of the Research Central Services (SCAI) of the University of Málaga. Financial support from the National Science Center of Poland (DEC-2015/19/B/ST5/00612, M.S.) is gratefully acknowledged. L.F. thanks Thomas Vives from the Ecole Nationale Supérieure de Chimie of Rennes, the Shimadzu and Chiral Technology companies for their support regarding the separation of the chiral molecule by

© 2022 The Authors. Angewandte Chemie International Edition published by Wiley-VCH GmbH

supercritical fluid chromatography (SFC). Funding for open access charge: Universidad de Málaga/CBUA

Conflict of Interest

The authors declare no conflict of interest.

Data Availability Statement

The data that support the findings of this study are available from the corresponding author upon reasonable request.

Keywords: Circularly Polarized Luminescence · Cycloparaphenylene · Lemniscular · Magnetic Moments · Raman Optical Activity

[1] K. Senthilkumar, M. Kondratowicz, M. Lis, P. J. Chmielewski, J. Cybińska, J. L. Zafra, J. Casado, T. Vives, J. Crassous, L. Favereau, M. Stępień, *J. Am. Chem. Soc.* **2019**, *141*, 7421–7427.
[2] For other chiral systems derived from macrocyclic oligophenylenes see: a) T. A. Schaub, E. A. Prantl, J. Kohn, M. Bursch, C. R. Marshall, E. J. Leonhardt, T. C. Lovell, L. N. Zakharov, C. K. Brozek, S. R. Waldvogel, S. Grimme, R. Jasti, *J. Am. Chem. Soc.* **2020**, *142*, 8763–8775; b) Y. Segawa, M. Kuwayama, Y. Hijkata, M. Fushimi, T. Nishihara, J. Pirillo, J. Shirasaki, N. Kubota, K. Itami, *Science* **2019**, *365*, 272–276; c) S. Nishigaki, Y. Shibata, A. Nakajima, H. Okajima, Y. Masumoto, T. Osawa, A. Muranaka, H. Sugiyama, A. Horikawa, H. Uekusa, H. Koshino, M. Uchiyama, A. Sakamoto, K. Tanaka, *J. Am. Chem. Soc.* **2019**, *141*, 14955–14960; d) J. Oniki, T. Moriuchi, K. Kamochi, M. Tobisu, T. Amaya, *J. Am. Chem. Soc.* **2019**, *141*, 18238–18245.
[3] a) R. Jasti, J. Bhattacharjee, J. B. Neaton, C. R. Bertozzi, *J. Am. Chem. Soc.* **2008**, *130*, 17646–17647; b) S. E. Lewis, *Chem. Soc. Rev.* **2015**, *44*, 2221–2304; c) Y. Segawa, A. Yagi, K. Matsui, K. Itami, *Angew. Chem. Int. Ed.* **2016**, *55*, 5136–5158; *Angew. Chem.* **2016**, *128*, 5222–5245; d) E. J. Leonhardt, R. Jasti, *Nat. Rev. Chem.* **2019**, *3*, 672–686.
[4] A. Bedi, O. Gidron, *Acc. Chem. Res.* **2019**, *52*, 2482–2490.
[5] E. Ehrenfreund, Z. Vardeny, O. Brafman, B. Horovitz, *Phys. Rev. B* **1987**, *36*, 1535–1553.
[6] C. Castiglioni, M. Tommasini, G. Zerbi, *Phil. Trans. R. Soc. A* **2004**, *362*, 2425–2459.
[7] P. Mayorga Burrezo, J. L. Zafra, J. T. López Navarrete, J. Casado, *Angew. Chem. Int. Ed.* **2017**, *56*, 2250–2259.
[8] P. W. Atkins, L. D. Barron, *Mol. Phys.* **1969**, *16*, 453–466.
[9] L. D. Barron, A. D. Buckingham, *Mol. Phys.* **1971**, *20*, 1111–1119.
[10] K. M. Spencer, T. B. Freedman, L. A. Nafie, *Chem. Phys. Lett.* **1988**, *149*, 367–374.
[11] L. A. Nafie, *Vibrational Optical Activity. Principles and Applications*, Wiley, Chichester, **2011**.
[12] H. P. J. M. Dekkers, in *Circular Dichroism. Principles and Applications* (Eds.: N. Berova, K. Nakanishi, R. W. Woody), Wiley-VCH, Weinheim, **2000**, pp. 185–211.
[13] J. P. Riehl, G. Muller, in *Comprehensive Chiroptical Spectroscopy: Instrumentation, Methodologies, and Theoretical Simulations, Vol. 1* (Eds.: N. Berova, P. L. Polavarapu, K. Nakanishi, R. W. Woody), Wiley-VCH, Weinheim, **2012**, pp. 65–90.
[14] T. Wu, J. Kapitán, V. Masek, P. Bour, *Angew. Chem. Int. Ed.* **2015**, *54*, 14933–14936; *Angew. Chem.* **2015**, *127*, 15146–15149.
[15] T. Wu, P. Bour, *Chem. Commun.* **2018**, *54*, 1790–1792.
[16] W. Hug, *Chem. Phys.* **2001**, *264*, 53–69.
[17] a) M. Fedorovsky, *Comput. Lett.* **2006**, *2*, 233–236. b) E. Ehrenfreund, Z. Vardeny, O. Brafman, B. Horovitz, *Phys. Rev. B* **1987**, *36*, 1535–1553.
[18] L. D. Barron, *Molecular Light Scattering and Optical Activity*, Cambridge University Press, Cambridge, **2004**.
[19] B. Nordén, A. Rodger, T. Dafforn, *Linear Dichroism and Circular Dichroism*, RSC Publishing, Cambridge, **2010**.
[20] M. Kasha, *Discuss. Faraday Soc.* **1950**, *9*, 14–19.
[21] C. Camacho, T. A. Niehaus, K. Itami, S. Irle, *Chem. Sci.* **2013**, *4*, 187–195.
[22] T. Iwamoto, Y. Watanabe, Y. Sakamoto, T. Suzuki, S. Yamago, *J. Am. Chem. Soc.* **2011**, *133*, 8354–8361.
[23] B. M. W. Langeveld-Voss, D. Beljonne, Z. Shuai, R. A. J. Janssen, S. C. J. Meskers, E. W. Meijer, J.-L. Brédas, *Adv. Mater.* **1998**, *10*, 1343–1348.

Manuscript received: May 12, 2022
Accepted manuscript online: July 3, 2022
Version of record online: July 14, 2022

© 2022 The Authors. Angewandte Chemie International Edition published by Wiley-VCH GmbH